Electronic Supplementary Material (ESI) for Chemical Communications.

Supplementary Material for

Co doping promotes the alkaline overall seawater electrolysis performance over $MnPSe_3$ nanosheets

Hao Zhang et al.

Experimental Section

Synthesis

Synthesis of CMPS and MPS: The preparation procedure used was obtained from the relevant literature with some modifications (*ACS Catalysis*, 2017, 7, 8159). First, a quartz glass ampule containing 0.1 g of $CoCl_2$, 1 g $MnCl_2$, phosphorus (Red phosphorus, 99.999 %, 0.5 g), and selenium (99.999 %, 1 g) was sealed under a high vacuum. Next, the mixture described above was transferred to the tube furnace and pyrolyzed at 700 °C for 24 h with a heating rate of 5 °C min^{-1}. After the samples were naturally cooled to room temperature, CMPS powder samples were obtained. The reference sample of $MnPSe_3$ (MPS) was prepared using the same synthetic route, except that no phosphorus source was involved.

Characterizations

The scanning electron microscopy (SEM, Quanta FEG 250) and transmission electron microscopy (TEM, Talos F200X) equipped with mapping of elements modules were performed to capture material morphological features. X-ray diffraction (XRD, Rigaku D/max 2500) instrumented with Cu Kα radiation and X-ray photoelectron spectroscopy (XPS, ESCALAB 250Xi, Thermo Scientific) with Al Kα radiation source were conducted to obtain crystalline structures and chemical composition, respectively. The cobalt doping amount was gathered through inductively coupled plasma (ICP, ICP-OES 8000DV, Optima). Meantime, the XPS spectra were calibrated to the C 1s peak at 284.5 eV before being analyzed.

Electrochemical tests

Electrochemical measurements, including HER and OER, were controlled via the electrochemical workstation (CHI 760E, Shanghai Chenhua) and three electrodes system with alkali media (1 M KOH, 1 M KOH + natural seawater). The carbon paper (HCP030N, 1.0 × 1.5 cm^2) loaded power ink as the work electrode, carbon rod (diameter, 6 mm) as the counter electrode, and Hg/HgO electrode as the reference electrode. The 5 mg catalyst materials (i.e., CMPS, MPS, Pt/C, and IrO_2) were dispersed in a mixture solution including 450 μL EtOH

and 50 μL Nafion through 30 min ultrasonic treatment. Then, 100 μL ink was applied dropwise to the carbon paper (1.0 × 1.0 cm^2) and dried at 60 °C in an oven. Electrochemical impedance spectroscopy (EIS) was conducted in the range of 0.01 Hz ~ 100 kHz with 300 mV overpotential applied to the OER and 200 mV overpotential applied to the HER. According to the formula of $E_{RHE} = E_{Hg/HgO} + 0.059 \times pH + 0.098$ V, the reversible hydrogen electrode (RHE) serves as the reference potential for all measurements. And all reported data have been performed with iR compensation.

DFT calculations

The Device Studio program provides a number of functions for performing visualization, modeling and simulation.[29,30] DS-PAW software was used for the calculations.[30] The exchange–correlation potential was treated by Perdew-Burke-Ernzerhof (PBE) generalized gradient approximation (GGA) functional. During the configuration optimization, the convergence tolerance was setted to be 1.0×10^{-5} eV for energy and 0.05 eV $Å^{-1}$ for force. The $MnPSe_3$ (11-3) model was constructed by 4 × 4 supercell with a vacuum region of 15 Å. Free energy for each reaction step was calculated as $G=E_{DFT}+E_{ZPE}-T\Delta S$, where E_{DFT} is the DFT calculated energy.

Figures and Table

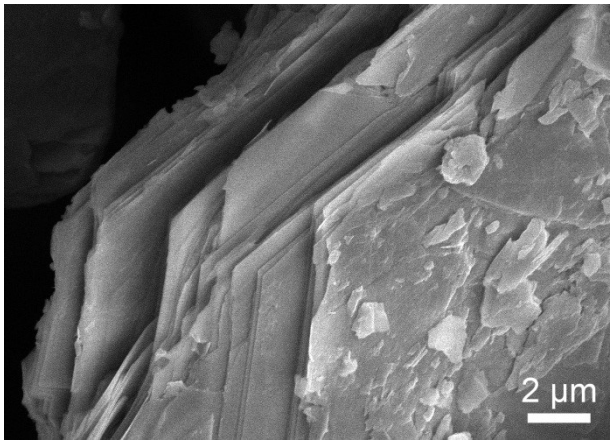

Figure S1. The SEM image of MPS.

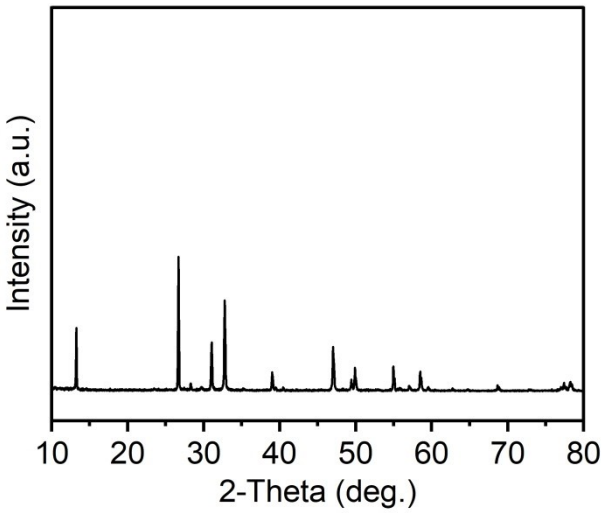

Figure S2. The XRD pattern of MPS.

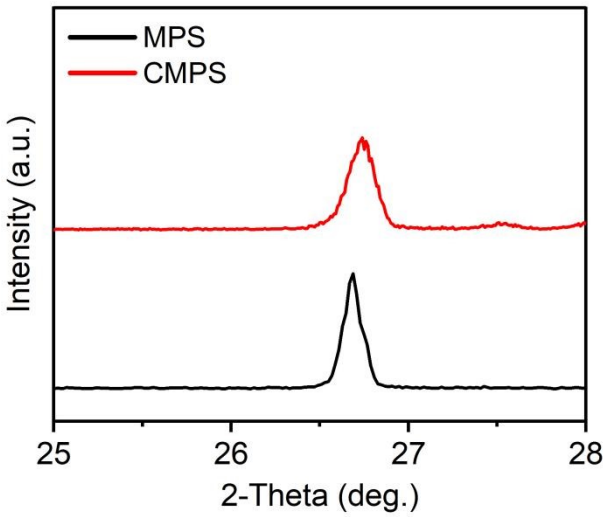

Figure S3. The enlarged XRD pattern of CMPS and MPS. As a result, the enlarged (006) diffraction peak at 26.7° of the CMPS is broadened and slightly shifted towards the high angle direction due to the Co atoms are doped at host Mn sites, indicating that Co doping induces distortion in the $MnPSe_3$ lattice. (J. Mater. Chem. A, 2023, 11, 6625; Chem. Eng. J. 2022, 450, 138358)

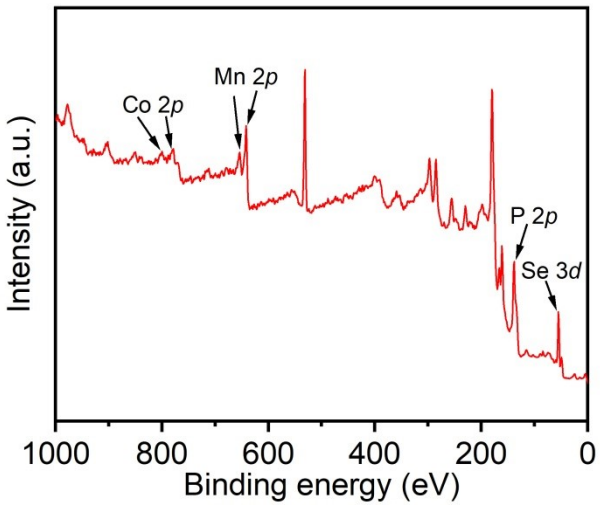

Figure S4. The survey scan spectrum of CMPS.

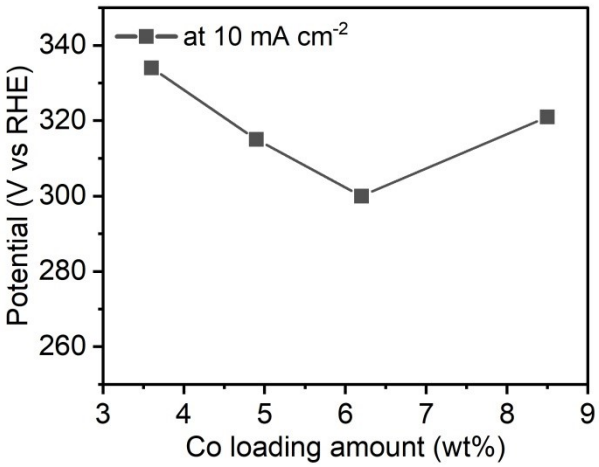

Figure S5. The potentials at 10 mA cm^{-2} for CMPS with different Co loading amount by ICP measurement.

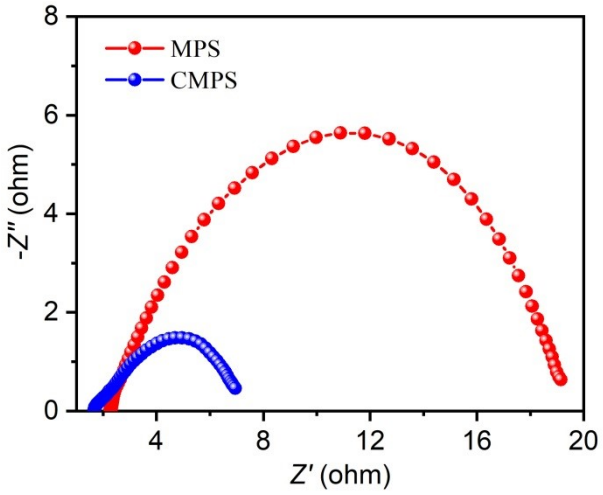

Figure S6. Nyquist plots with 300 mV overpotential.

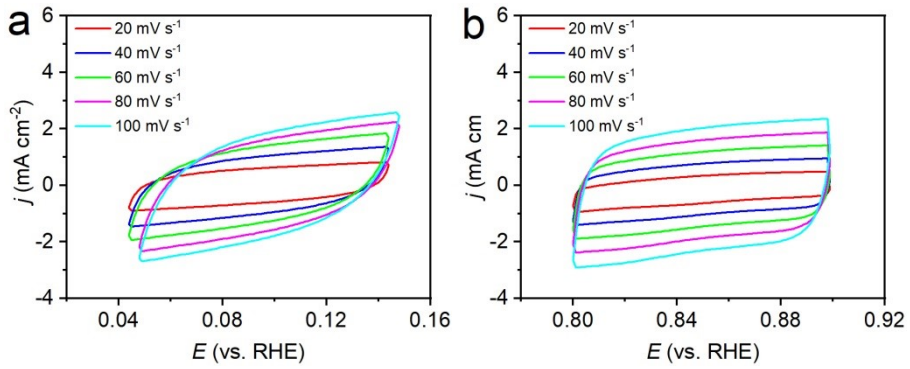

Figure S7. CV curves of (a) MPS and (b) CMPS at various scan rates from 20-100 mV s^{-1} in the range of the non-faradaic region.

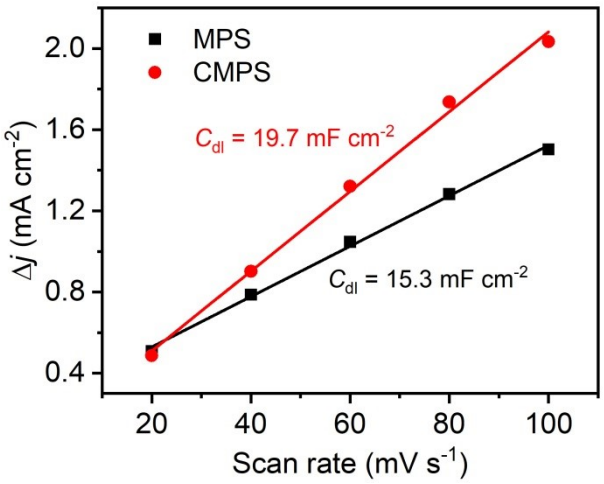

Figure S8. Electrochemical surface areas of the CMPS and MPS.

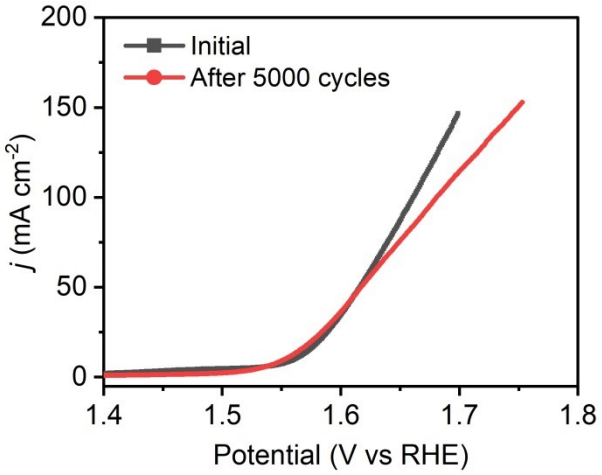

Figure S9. LSV curves of CMPS after 5,000 cycles at a scan rate of 50 mV s^{-1}.

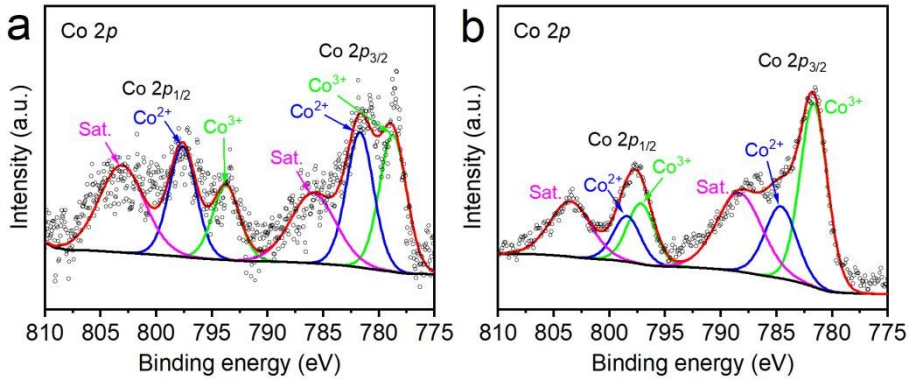

Figure S10. The high-resolution XPS spectra of Co 2p of CMPS before (left) and after (right) the OER stability test. It is found that more high valence state Co^{3+} species are observed due to the formation of Co-(oxy)hydroxides via electro-oxidation, i.e., the Co^{3+}/Co^{2+} ratio was increased from 1.18 before the reaction to 1.87 (J. Colloid Interface Sci. 2023, 645, 724). Previous research has shown that these generated (oxy)hydroxides derived from surface reconstruction are real reactive species, which plays a positive role in catalyst activity and stability for the OER (J. Colloid Interface Sci. 2023, 645, 724; Int. J. Hydrog. Energy 2023, 48, 5080).

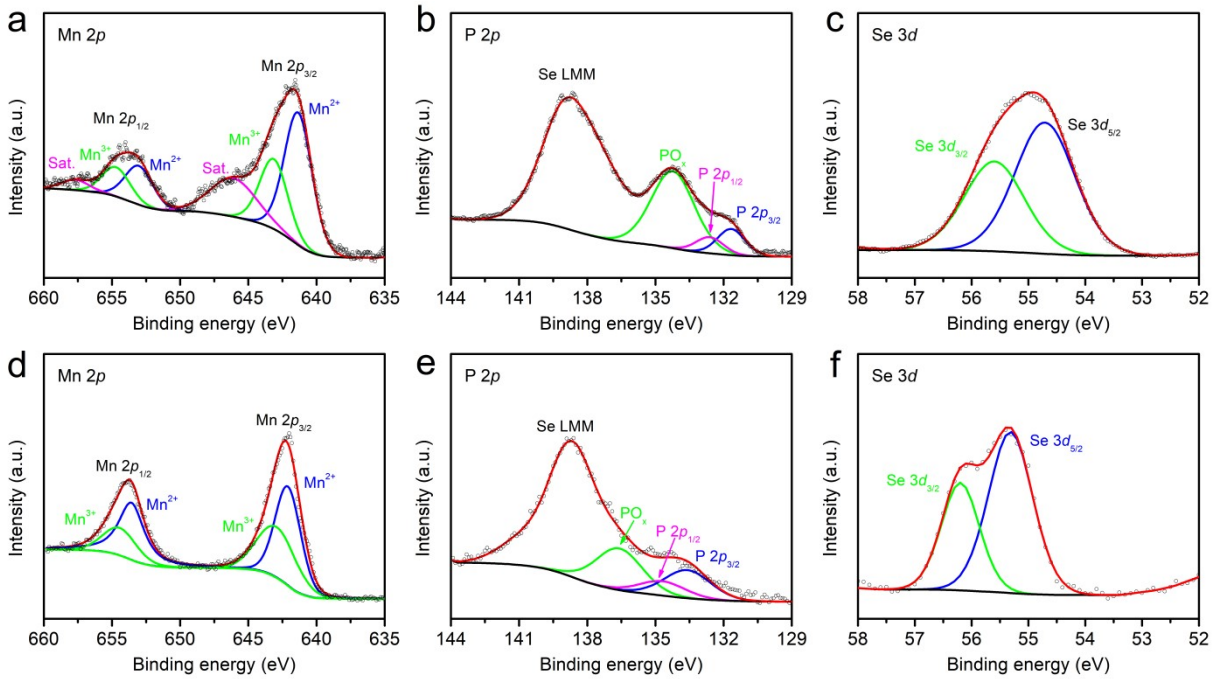

Figure S11. The high-resolution XPS spectra of (a, d) Mn 2p, (b, e) P 2p, and (c, f) Se 3d of CMPS before (top) and after (bottom) the OER stability test. Similar to the case of Co 2p, Mn 2p also showed an increase in Mn^{3+}/Mn^{2+} ratio from the original 0.58 to 0.72 after OER stability tests, implying the formation of an amorphous layer of Mn-hydroxide on the surface in reaction process (ACS Energy Lett. 2018, 3, 9, 2150-2158). For P 2p and Se 3d, the core peaks of them shifted to higher binding energy (~2.0 eV, ~0.6 eV), suggesting a much stronger oxidation on the surface of the catalyst under OER conditions (Chem. Eng. J. 2020, 398, 125660; Adv. Mater. 2021, 33, 2007523; Chem. Eng. J. 2021, 420, 130461).

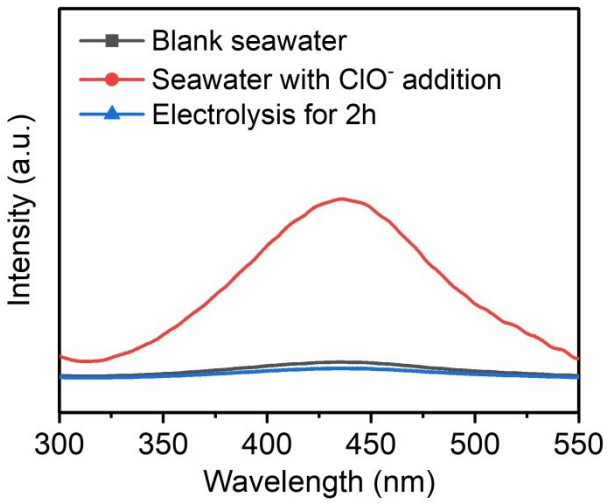

Figure S12. UV-vis absorption spectra of the electrolytes (0.1 mL) taken from various electrolysis conditions. It is found that no ClO^- generation is detected under a potential of 1.67 V vs RHE over 30 h. First, the chloride electro-oxidation reaction, i.e., $2Cl^- \rightarrow Cl_2 + 2e^-$ (E^o = 1.36 V, pH = 0) and $Cl^- + 2OH^- \rightarrow ClO^- + H_2O + 2e^-$ (E^o = 0.89 V, pH = 14), is an important competing side reaction with OER on anode, and this reaction is capable of producing several chlorine species, e.g., Cl_2, ClO^-. (Angew. Chem.Int. Ed. 2022, 61, e202210753;) All electrochemical tests in this work were performed in alkaline seawater (1 M KOH + natural seawater, pH ≈ 13.8), and the generated Cl_2 can react with OH^-, $Cl_2 + 2OH^- \rightarrow Cl^- + ClO^-$, so that ClO^- species can be used as evidence of whether Cl^- oxidation reactions are occurring or not. (Nat. Energy, 2020, 5,367-377; Nat. Commun. 2021, 12, 4182) Furthermore, compared to the lower thermodynamic potential of 1.23 V vs RHE for electrochemical water splitting, the oxidation potential of the chlorine electro-oxidation reactions was up to 1.72 V in alkaline seawater. (Nat. Commun. 2021, 12, 4182) However, after 30 h of stability measurement of the CMPS by applying a 1.67 V at 100 mA cm^{-2}, it was found that no ClO^- generation was detected, suggesting that the CMPS has better OER selectivity.

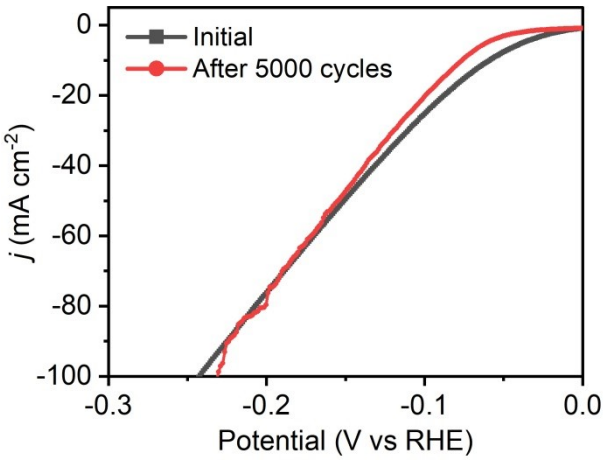

Figure S13. LSV curves of CMPS for HER initially and after 5,000 cycles at a scan rate of 50 mV s^{-1}.

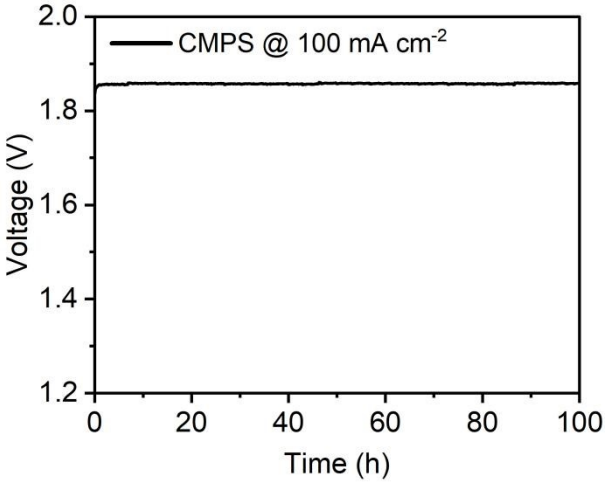

Figure S14. Chronoamperometry stability test at 100 mA cm^{-2} for CMPS.

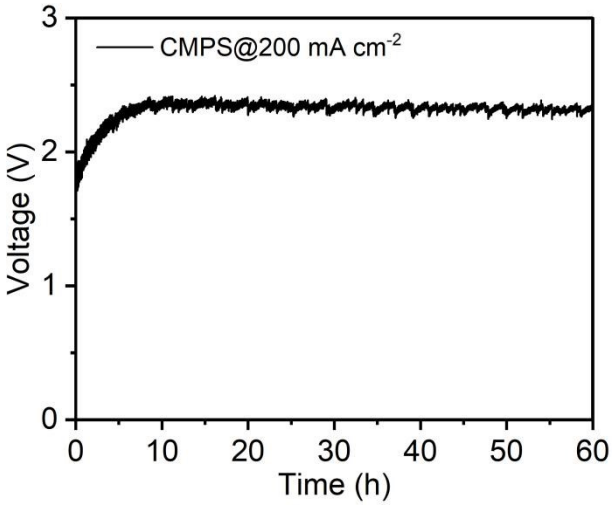

Figure S15. Chronoamperometry stability test of CMPS at 200 mA cm^{-2} for 60 h.

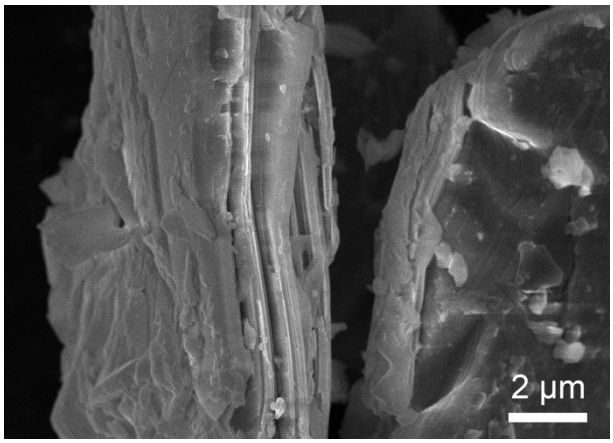

Figure S16. SEM image of the CMPS after the stability test.

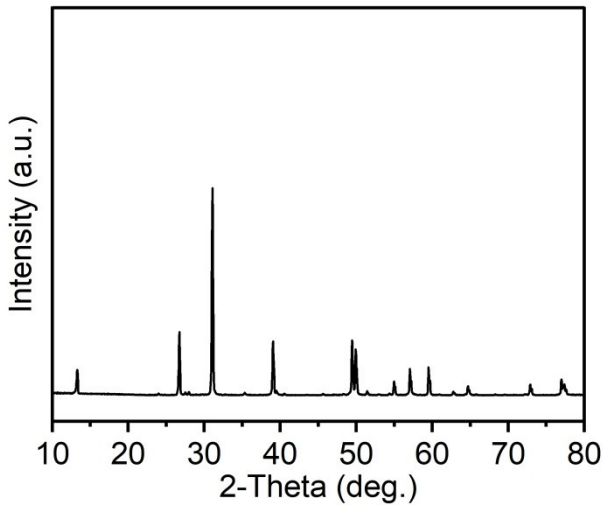

Figure S17. XRD pattern of the CMPS after the stability test. Through comparing the XRD characterization before and after stabilization (Figures 2a and S16), it was found that the CMPS catalyst changed some of the peak intensities after seawater electrolysis of long period and no new crystal structures were observed, which could be attributed to the formation of different catalytic species on the surface of the CMPS catalyst through oxidation.

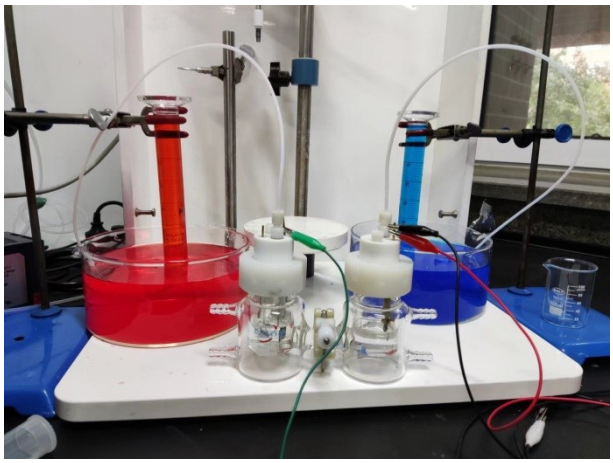

Figure S18. The gas collection device of water splitting in 1.0 M KOH + seawater solution.

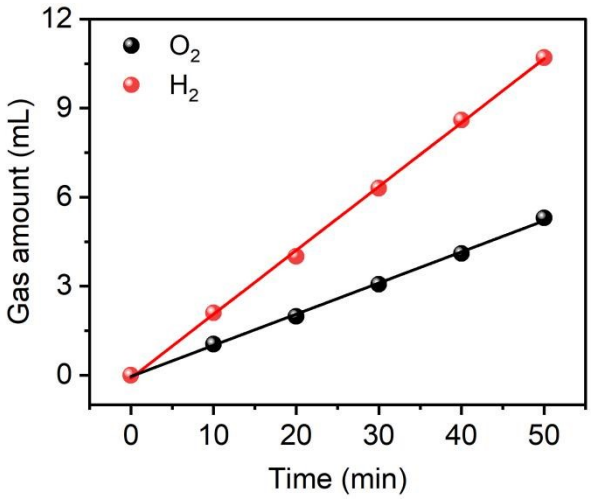

Figure S19. Generated volume of H_2 and O_2.

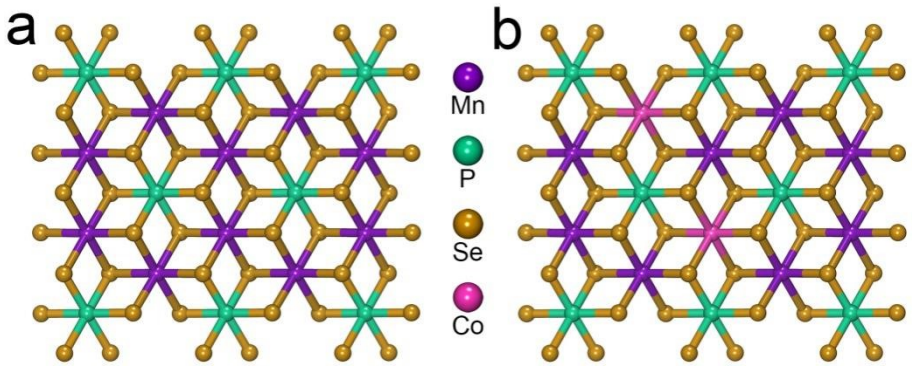

Figure S20. The theoretical models of (a) MPS and (b) CMPS.

Table S1. Comparison of alkaline seawater splitting performances for CMPS with other reported electrocatalysts.

Catalysts	Electrolyte	Potential @ current density (V @ mA cm^{-2})	Stability (mA cm^{-2}, hours)	Reference
CMPS	1 M KOH + seawater	1.82 @ 100	100, 100	This work
Mo-CoP_x/NF	1 M KOH + seawater	2.16 @ 100	100, 100	Mater. Today Nano, 2022, 18, 100216
1D-Cu@Co-CoO/Rh	1 M KOH + 0.5 M NaCl	1.9 @ 100	10, 12	Small, 2021, 17, 2103826
NiCoHPi@Ni_3N/NF	1 M KOH + 0.5 M NaCl	1.86 @ 100	200, 40	ACS Appl. Mater. Interfaces. 2022, 14, 22061
Ni_3S_2-MoS_2-Ni_3S_2/NF	1 M KOH + seawater	1.82 @ 100	100, 100	Electrochimica Acta, 2021, 390, 138833
Ni_2P-Fe_2P/NF	1 M KOH + seawater	1.811 @ 100	100, 48	Adv. Funct. Mater., 2021, 31, 2006484
RuNi-Fe_2O_3/IF	1 M KOH + seawater	1.73 @ 100	100, 100	Chinese J. Catal., 2022, 43, 2202
CoP_x@FeOOH/NF	1 M KOH + seawater	1.71 @ 100	500, 80	Appl. Catal. B Environ. 2021, 294, 120256
NF@$NiMoO_4$/N/P	1 M KOH + 0.5 M NaCl	1.70 @ 100	100, 24	J. Electrochem. Soc., 2022, 169, 046511
CNC-MO & CNC-MS	1 M KOH + 0.5 M NaCl	1.61 @ 100	100, 120	Nano Energy, 2021, 87, 106160

The assembled CMPS//CMPS alkaline seawater electrolyzer can be can be stabilized for 100 h at 100 mA cm^{-2} current densities and applied potential of ~1.82 V, and it was discovered that this CMPS electrocatalys were on par with or even superior to those of these reported catalysts in recent years in **Table S1**.

Also, we summarized the recently reported the ternary transition metal tri-chalcogenides (TMTCs)-based materials to compare the difference of them. For HER, the as-synthesized

CMPS possessed a lower overpotentials of 59 mV at 10 mA cm^{-2} in alkaline seawater, which is better than the exfoliated layered $MnPSe_3$ (640 ± 87 mV in 0.5 M H_2SO_4; 992 ± 56 mV in 1 M KOH; Adv. Funct. Mater. 2018, 29, 1805975), $MoS_{0.94}Se_{0.53}$ (150 mV in 0.5 M H_2SO_4; Adv. Mater. 2016, 28, 1427), Few-layered $FePS_3$ (108 ± 2 mV in 0.5 M H_2SO_4; 337 ± 4 mV in 1 M KOH; ACS Energy Lett. 2016, 1, 367), and $BiPS_4$ (400 ± 138 mV in 0.5 M H_2SO_4; ACS Appl. Mater. Interfaces 2017, 9, 12563). For OER, the CMPS's catalytic activity (300 mV at 10 mA cm^{-2} in alkaline seawater) is also comparable to the reported materials, such as $NiPS_3$ (~840 mV in 1 M KOH; ACS Appl. Mater. Interfaces 2017, 9, 12563) and $FePSe_3$ (~370 mV in 1 M KOH; ACS Catal. 2017, 7, 8159-8170).